

# Flame Acceleration and Deflagration-to-Detonation Transition in Three-Dimensional Rectangular Channel

M.F. Ivanov<sup>1</sup>, A.D. Kiverin<sup>1</sup>, M.A. Liberman<sup>1,2,3</sup>, I.S. Yakovenko<sup>1</sup>

<sup>1</sup>Joint Institute for High Temperatures, Russian Academy of Science, Izhorskaya 13, Bd. 2  
Moscow 125412, Russia

<sup>2</sup>Department of Physics and Astronomy, Uppsala University, Box 530, SE-751 21, Uppsala  
Sweden

<sup>3</sup>Moscow Institute of Physics and Technology, Institutskii per. 9, Dolgoprudnyi, Moskovsk.  
obl.,141700, Russia

## 1 Introduction

This paper discusses the features of flame acceleration and deflagration-to-detonation transition (DDT) in the confined volumes (channels). Over the past decades this problem has been intensively investigated since an understanding of how DDT occurs is important for industrial safety and because of its potential application for micro-scale propulsion and power devices. Over the years DDT was one of the least understood processes in hydrodynamics, nonlinear physics, combustion science and astrophysics in spite of its extreme importance. Significant efforts have been devoted to understand the nature of the flame acceleration and mechanism of DDT. However DDT mechanism remained unclear until the recent works [1, 2, 3] devoted to disclose the phenomena origins using theoretical analysis, analysis of DDT experiments [4, 5] and 2D computations utilizing detailed models for chemical kinetics and transport phenomena. It was shown that the flame acceleration in tubes with no-slip walls is a defining factor in creating the right conditions for DDT. The dynamics of the whole DDT process may vary depending on the upstream flow field structure generated by the accelerating flame, so that for every combustible mixture there are a critical width of the channel, for which dynamics of flame acceleration changes [1-3]. Above this critical width the flame evolves in three stages and below it flame evolves in two stages, which is confirmed by the DDT experiments in hydrogen-oxygen and ethylene-oxygen [4, 5, 6]. Most of previous computations were carried out for two-dimensional case where the in-channel flow was assumed to be planar. In the present work a 3D simulations of the flame acceleration and DDT in a three-dimensional rectangular channel were performed to investigate the features of 3D phenomenon compared to 2D one.

## 2 Problem Setup

The high resolution simulations were used to model a flame ignited near the closed end and then propagating to the open end of the channel, filled with stoichiometric hydrogen-oxygen mixture at initial temperature  $T_0=300\text{K}$  and pressure  $p_0=1\text{atm}$ . To understand the features of the flame acceleration in three-dimensional setup compare with two-dimensional both 2D and 3D computations were carried out. The computations solved two- and three-dimensional, time-dependent, reactive

Navier-Stokes equations for compressible flow including the effects of viscosity, thermal conduction, molecular diffusion, the real equation of state and detailed chemical kinetics for the reactive species  $H_2$ ,  $O_2$ ,  $H$ ,  $O$ ,  $OH$ ,  $H_2O$ ,  $H_2O_2$ , and  $HO_2$  with subsequent chain branching and energy release. The real equations of state for the fresh mixture and combustion products were taken with the temperature dependence of the specific heats and enthalpies of each species borrowed from the JANAF tables and interpolated by the fifth-order polynomials. The transport coefficients were calculated from the first principles using the Lennard-Jones potential. Coefficients of the heat conduction of  $i$ -th species  $\kappa_i = \mu_i c_{p,i} / Pr$  are expressed via the kinematic viscosity  $\mu_i$  and the Prandtl number, which is taken  $Pr \approx 0.71 \div 0.75$ . The reaction scheme for a stoichiometric  $H_2$ - $O_2$  mixture used in the simulations has been proved to be adequate to complete chemical kinetic scheme. The computed thermodynamic, chemical, and material parameters using this chemical scheme are in a good agreement with the flame and detonation wave characteristics measured experimentally. The high resolution numerical simulation and computational method used are described in [2, 3]. Its validation, the convergence and resolution tests with the meshes taken to resolve the structure of the flame front up to 64 computational cells per flame width are presented in [2, 3].

### 3 Flame evolution

The overall picture of the flow, the flame evolution and the transition to detonation computed for the channel of square cross-section with width  $D=5\text{mm}$ , is shown in figure 1. The physical times in milliseconds shown for each frame in Fig. 1 are not evenly spaced but clustered to reveal the most important details of the flame acceleration and the transition to detonation. The shape of the flame depends on the small perturbations imposed at the beginning.

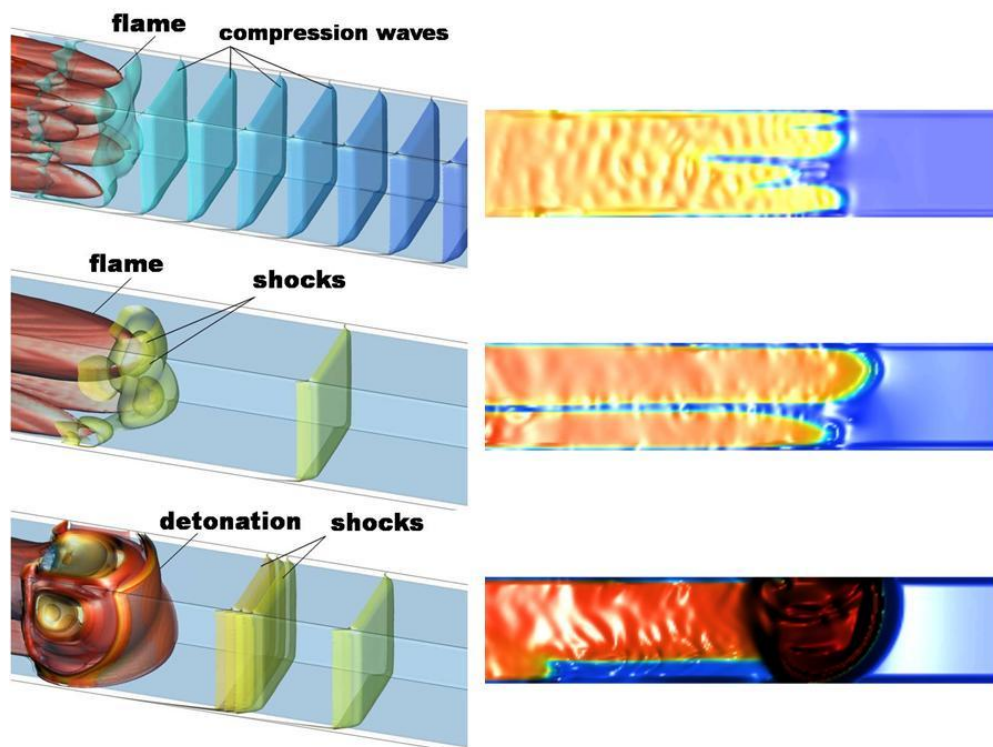


Figure 1. Flame structure and pressure waves in its vicinity at sequential times (200, 375 and 430us) in square-cross channel of  $D=5\text{mm}$ . Right part represents two-dimensional crosses.

In 2D case the main direction of flame propagation is associated with the walls, and initially planar flame evolves into the tulip-shaped or single-mode flame which leading tips are moving along the walls (see. e.g. figure 1 in [2]). In 3D case the unperturbed planar flame aims to move along the edges between the channel walls and only in case of non-regular initial perturbation it evolves into the non-symmetrical shape with tips moving in the bulk far from the walls. For typical flame shapes (see figure 2) one can see that initial perturbations tend to destroy the symmetrical shapes specified by geometrical features of the channel, however the overall dynamics of the flame acceleration remains almost the same. Moreover the dynamics is similar to that obtained for 2D case except the higher acceleration rate associated with additional degree of freedom. Figure 3 shows the evolution of the flame speed and peak pressure throughout the process of the flame acceleration and DDT computed for 2D and 3D cases.

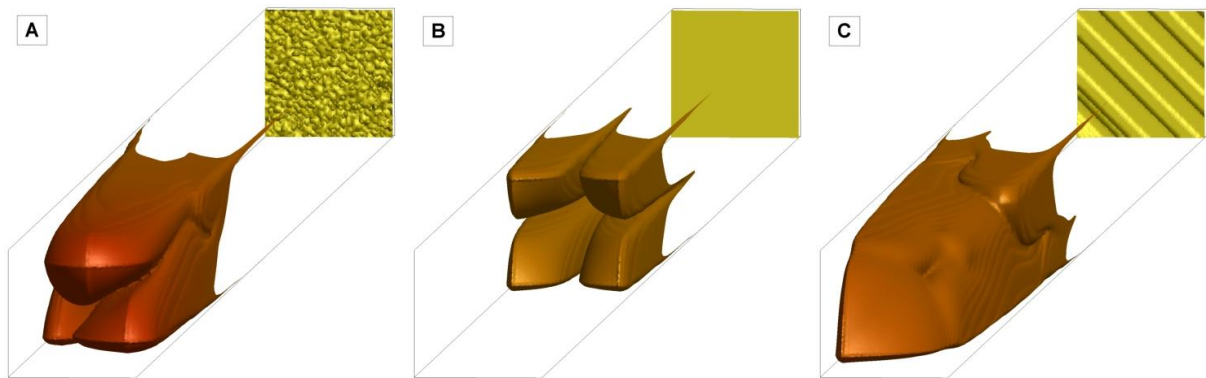


Figure 2. Flame structure (orange surfaces) depending on the initial perturbations (yellow surfaces). A - case of random perturbation, B - case of the initially unperturbed planar flame, C - case of regular perturbation.

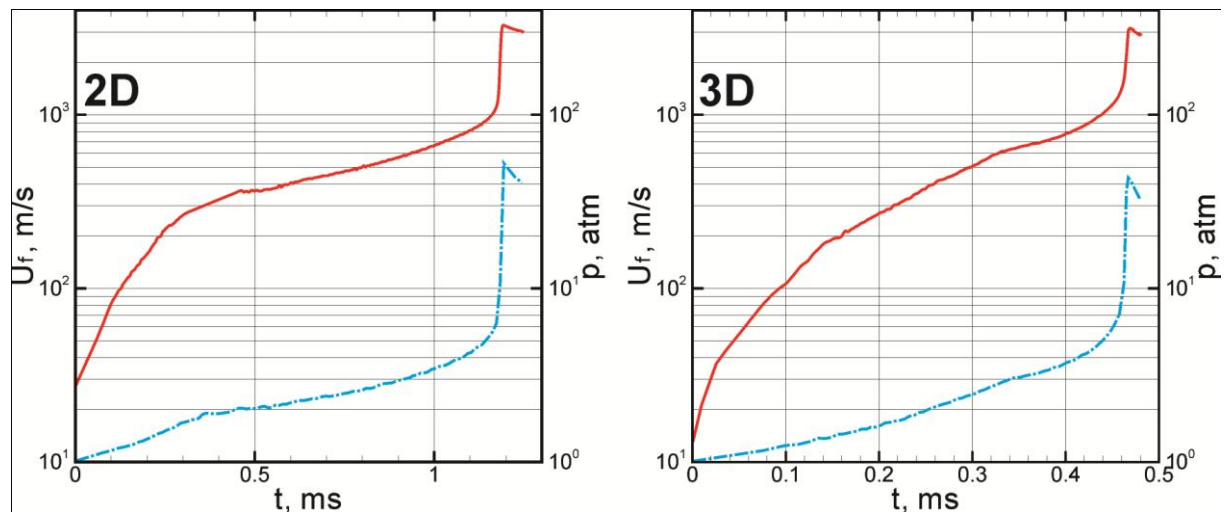


Figure 3. Computed flame velocity (solid lines) and peak pressure (dash-dotted lines) time dependences for 2D and 3D channels of  $D=5\text{mm}$ .

For both 2D and 3D cases the velocity-time dependence plots demonstrate the same feature of several distinctive stages of the flame acceleration: (0) initial stage of flame expansion out from the ignition zone; (1) the stage of exponential increase of the flame velocity; (2) the stage when the rate of acceleration decreases compared with the previous nearly linear stage; (3) the sharp increase of the flame velocity and actual transition to detonation. The evolution of the process in 3D case appears to be faster mainly because of the shorter stage (1) and as a result more violent conditions at the beginning of the stage (3) which determines the DDT [2, 3].

#### 4 Flame acceleration, shocks formation and mechanism of DDT

A propagating flame initiated near the closed end of the channel controls the flow forming ahead of it, which results in the flame acceleration compatible with the physical boundary conditions. When the flame is initiated near the closed end, the expansion of the high temperature burned gas induces an outward flow of the unburned mixture with the velocity  $u = (\Theta - 1) \cdot U_{f0}$  ahead of the flame front while the flame propagates with the velocity  $U_f = \Theta \cdot U_{f0}$  in the laboratory reference of frame [7], where  $U_{f0}$  is the normal velocity of laminar flame at the ambient conditions and  $\Theta = \rho_u / \rho_b$  is the density ratio of the unburned  $\rho_u$  and burned  $\rho_b$  gases, respectively. Because of the wall friction the velocity in the upstream flow is maximal at the axis and it vanishes at the channel walls. The average velocity is approximately constant in the bulk and drops to zero within a thin boundary layer. Every part of the flame front moves with respect to the unreacted mixture in the upstream flow with normal velocity  $U_{f0}$  and simultaneously it is drifted with the local velocity of the flow ahead of the flame. Thus, the flame shape is defined by the relative motion of different parts of the flame front. As the flame front advances into a non-uniform velocity field, the flame surface stretches repeating to a large extent the shape of the velocity profile in the upstream flow, therefore the flame surface increases. The stretched flame consumes fresh fuel over a larger surface area which results in an increase in the rate of heat release per unit projected flame area. The increase in the rate of heat release due to the flame stretching gives rise to a higher volumetric burning rate, and a higher effective burning velocity based on the average heat release rate per frontal area of the stretched flame sheet. A higher burning velocity results in an enhancement of the flow velocity ahead of the flame, which in turn gives rise to a larger gradient field and enhances the flame stretching, and so on. In this way a positive feedback coupling is established between the upstream flow and the burning velocity as the flame is stretched due to non-uniform velocity profile in the upstream flow. Such a feedback determines exponential flame acceleration at stage (1) where combustion wave velocity can be presented as  $U_f = \Theta U_{f0} \cdot \exp(\alpha U_{f0} t / D)$ , where  $\alpha$  is a numerical factor of the order of unity. After a short time during the stage (1) the backward edges of the flame front (flame skirt) are stretched along the walls within the boundary layer. The parts of the flame surface, which come close to the walls of the channel, quench on the walls. As a result one can observe the reduction of the rate of flame surface increase and corresponding value of flame acceleration. Because of short time of the first stage the flame acceleration during the first stage is nearly constant with accuracy of the first order terms of series expansion in  $L_f / D \ll 1$ , where  $L_f$  is a flame thickness. Therefore, during the next second stage the flame velocity increases as  $U_f \propto t^n$ , where  $n$  is in the range  $0 < n < 1$ .

The accelerating flame acts as a piston producing compression waves in the unreacted gas. The time and the coordinate where the compression wave steepens into a shock wave are determined by the condition that the velocity  $u(x, t)$  in the Riemann solution for a compression wave becomes a multi-valued function [8]. This condition defines the distance between the flame ( $x = X_f$ ) and the coordinate ( $x = X_{SW}$ ) where the compression wave steepens into a shock. At stage (1) it is estimated as  $(X_{SW} - X_f) \sim (5 \div 7)D$  and the shock is forming far ahead the flame front (see figure 1a). It can be shown [1-3] that for a piston moving with the velocity-time dependence taking place at the stage (2) the Riemann solution for a simple wave  $u(x, t)$  is multi-valued everywhere for any values of  $0 < n < 1$ . This means that the compression wave produced by the flame steepens into the shock directly on the surface of the flame (see figure 1b). Specific value of  $0 < n < 1$  does not matter since we are interested only in the location where the shocks are formed.

In contrast to a stationary flame, the flow with the accelerating flame is not isobaric. In the latter case pressure is growing at about the same rate as the flame velocity. From the time when the compression waves steepen into the shock close to the flame front, the unreacted mixture of considerably higher density compressed in the shock starts entering the flame front and produces a narrow pressure peak on the scale of the flame width (see pressure profile in the vicinity of the flame front on figure 4), which amplitude grows gradually due to the combustion of larger amount of compressed mixture behind the shocks running out from the reaction zone during this stage. After the

flow speed ahead the flame is accelerated up to the local sound speed the shocks do not run away from the reaction zone where they were born and the pressure peak is localized directly in the reaction zone. Eventually, the pressure peak becomes strong enough to affect reactions. The increase of the pressure enhances reaction rate and the heat release in the reaction zone creating a positive feedback coupling between the pressure pulse and the heat released in the reaction. It results in more violent pressure peak increase and formation of the shock strong enough for transition to detonation.

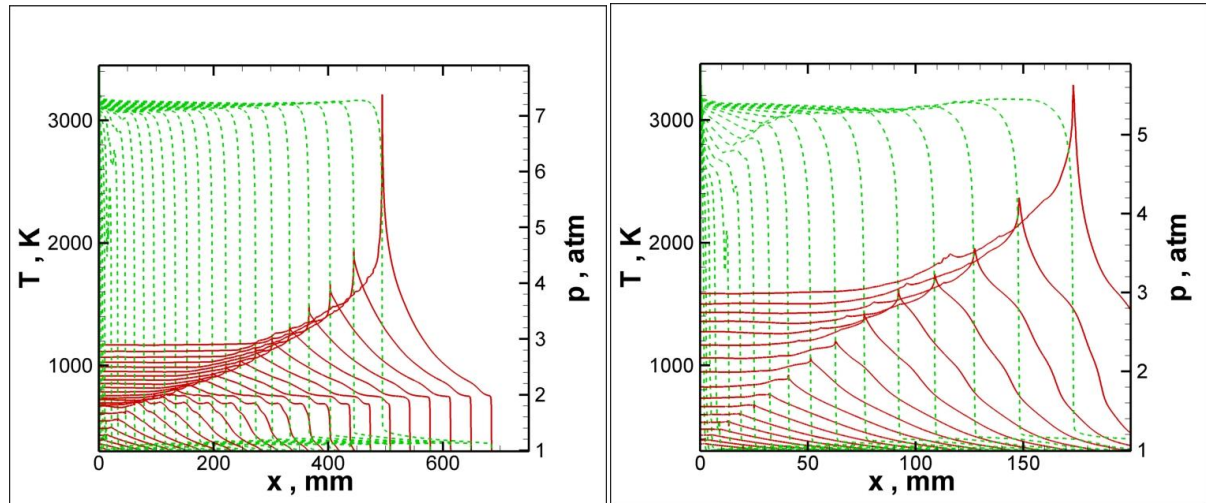


Figure 4. Temperature (dashed lines) and pressure (solid lines) profiles corresponding to leading point of the flame front represent the flame structure and the pressure peak formation; 2D case,  $D=5\text{mm}$ , time instants are from  $t_0=30\mu\text{s}$ ,  $\Delta t=50\mu\text{s}$ ,  $t_f=1180\mu\text{s}$ . 3D case,  $D=5\text{mm}$ , time instants are from  $t_0=50\mu\text{s}$ ,  $\Delta t=25\mu\text{s}$ ,  $t_f=450\mu\text{s}$ .

## 5 Conclusions

The insight into how DDT occurs and what is the mechanism of DDT was obtained by analyzing a series of high resolution multidimensional numerical simulations with a detailed chemical reaction model. DDT was simulated resolving the scales ranging from the size of the system to the scales much smaller than the flame thickness. It was shown that the exponentially growing pressure peaks, which start-up the transition to detonation, arise from the compression waves when they steepen into the shocks close to the flame front. So the DDT in channels is entirely determined by the features of the flame acceleration in the channel with no-slip walls. Though some details of the dynamics of the flame acceleration are different the mechanism of DDT appears to be the same in 2D and 3D rectangular channels. In 3D case the run-up distance is shorter because of the higher acceleration rate determined by the features of three-dimensional evolution of the non-stationary flow. The qualitative pattern of flame acceleration and DDT is independent on the specific features of initial conditions and geometry of the channel.

## References

- [1] Liberman MA., Ivanov MF., Kiverin AD., Kuznetsov MS., Chukalovsky AA., Rakhimova TV., Deflagration-to-detonation transition in highly reactive combustible mixtures, (2010) *Acta Astronautica*, 67: 688.
- [2] Ivanov MF, Kiverin AD, Liberman MA. (2011) Flame acceleration and DDT of hydrogen-oxygen gaseous mixtures in channels with no-slip walls, *Int. J. Hydrogen Energy*, 36: 7714.

- [3] Ivanov MF, Kiverin AD, Liberman MA. (2011) Hydrogen-oxygen flame acceleration and transition to detonation in channels with no-slip walls for a detailed chemical reaction model, *Phys. Rev. E.*, 83: 056313.
- [4] Kuznetsov M., Liberman M., Matsukov I., (2010) Experimental study of the preheat zone formation and deflagration-to-detonation transition, *Combust. Sci. Tech*, 182: 1628.
- [5] Kuznetsov M, Alekseev V, Matsukov I, Dorofeev S. (2005) DDT in a smooth tube filled with a hydrogen-oxygen mixture, *Shock Waves*, 14: 205.
- [6] Wu M, Burke MP, Son SJ, Yetter RA. (2007) Flame acceleration and the transition to detonation of stoichiometric ethylene-oxygen in microscale tubes, *Proceedings of the Combustion Institute*, 31: 2429.
- [7] Zel'dovich YaB., Barenblatt GI., Librovich VB., Makhviladze GM., *The Mathematical Theory of Combustion and Explosion*, Plenum, New York, 1985.
- [8] Landau L.D., Lifshitz E.M., *Fluid Mechanics*, Pergamon Press, Oxford, 1989.